Multiphonon interband absorption involving free electrons and phonons in n-type InAs

A. M. Danishevskiĭ, E. Yu. Perlin, and A. V. Fedorov

(Submitted 23 January 1987)
Zh. Eksp. Teor. Fiz. **93**, 1319–1328 (October 1987)

An investigation has been made of the generation of electron–hole pairs in n-type InAs in the region of the "tail" of three-photon fundamental absorption. The rates of generation of pairs W and the linear–circular dichroism parameter $\Lambda = W_l / W_c$ have been determined as a function of the energy deficit $\Delta_3 = E_g - 3\hbar\omega$ (E_g is the band gap). The dependence of $W_{l,c}$ on the intensity I of the pump radiation (which was linearly or circularly polarized radiation from a pulsed CO_2 laser) has been determined for different values of Δ_3 and of the free-carrier density n_0. A consistent interpretation of the experimental results is based on a proposed theory which includes a calculation of the probabilities of two types of indirect three-photon transitions. The deficit Δ_3 is balanced by a longitudinal optical phonon or by the kinetic energy of a free electron. For $n_0 \lesssim 10^{16}$ cm^{-3} the main role is played by the first of these mechanisms, whereas the second predominates for $n_0 \gtrsim 10^{17}$ cm^{-3}. In the intermediate range of carrier densities these two mechanisms make comparable contributions to the rates of generation of electron–hole pairs. The nature of the dependence of W on I, which differs for linear and circular polarizations of the pump radiation, is governed largely by the departure from equilibrium of the electron and phonon subsystems due to the action of high-power radiation.

1. INTRODUCTION

The processes occuring when electron–hold (EH) pairs are excited in semiconductors by high-intensity radiation of photon energy $\hbar\omega$ less than the band gap E_g are so many and so complex that they are still being actively investigated. The present paper reports a study of multiphoton transitions between the valence band v and the conduction band c with extrema at the center of the Brillouin zone in the case when

$$0<\Delta_s=E_g-s\hbar\omega\ll\hbar\omega \tag{1}$$

(s is the number of photons). We shall consider two types of indirect multiphonon transitions in which the deficit Δ is compensated by the kinetic energy of a free electron or by the absorption of an optical phonon. In addition to qualitatively new effects, which will be mentioned below, these processes retain certain features of direct multiphonon transitions near the fundamental absorption edge, such as the relatively lower probabilities of transitions involving an even number of photons and also the existence of complex polarization characteristics. In particular, the probabilities $W^{(s)}$ of s-photon transitions in the case of linearly polarized and circularly polarized light are different even for cubic crystals with a quasispherical energy band spectrum. Such linear–circular dichroism (LCD) is characterized by a parameter $\Lambda^{(s)} = W_l^{(s)}/W_c^{(s)}$. The parameter $\Lambda^{(2)}$ is close to unity for semiconductors.[1,2] For $s > 2$, the situation changes qualitatively, because in this case the transitions at $\mathbf{k} = 0$ are forbidden for circularly polarized light in the two-band model.[3] The probabilities of such forbidden transitions are calculated in Refs. 4 and 5 for arbitrary values of s. A strong LCD was reported in Refs. 6–8 above the three-photon absorption edge. According to the theoretical predictions, a rapid fall $\Lambda^{(3)}$ was observed when the deficit increased in the range $(-\Delta_3) > 0$.

An investigation of the LCD plays an important role in the identification of s-photon transitions. In particular, a large value of $\Lambda^{(s)}$ in the region of the "tail" of an s-photon transition (Sec. 2) is evidence of indirect multiphoton transitions involving s photons. An important feature of indirect multiphoton transitions considered in the present investigation is a change in the distribution functions of the phonons stimulating the process and of free electrons under the action of a high-power radiation generating nonequilibrium EH pairs. This significantly affects how the probabilities $W^{(s)}$ depend on the radiation intensity I, temperature T, etc. Consequently, the experimentally determined $W^{(s)}(I)$ grows faster than I^s. Then, in the case of linearly polarized radiation the probability $W^{(s)}$ increases with I usually more slowly than in the case of circularly polarized radiation. Dependences of this type, deduced from various theoretical ideas (see Secs. 3 and 4), support the proposed mechanisms of indirect multiphoton transitions.

These effects can be observed and investigated most conveniently in materials exhibiting not two-photon but three-photon transitions characterized by a strong LCD. A very suitable material is crystalline n-type InAs for which the value of E_g can be varied (by altering the temperature) in such a way that it is either greater or smaller than three CO_2 laser photons. Moreover, the relatively small values of E_g and of the effective masses of electrons m_c and light holes m_l (the mass of heavy holes will be denoted by m_h) in InAs ensure that the probabilities of multiphoton transitions are higher than in wide-gap materials.

2. NONLINEAR ABSORPTION IN n-TYPE InAs: EXPERIMENTS

The measurements were carried out using two light beams directed at an angle of $\sim 1°$ relative to one another in a crystal of n-type InAs.[1] The stronger of the beams was used as the pump radiation generating EH pairs, whereas the other (weaker) was used as the probe radiation. Both beams were generated by a pulsed CO_2 laser ($\lambda = 10.6$ and 9.5 μm). The intensity of the probe beam J_{pr} was less than 1% of

 0038-5646/87/100747-07$04.00 © 1988 American Institute of Physics

the intensity of the pump beam I. Interference of the probe beam was avoided by ensuring that the samples were beveled at an angle of $\sim 4°$.

The pump radiation was interrupted by a low-frequency chopper and the result of modulation of the probe radiation flux $\Delta J_{pr} = J^0_{pr} - J_{pr}$ was detected. Then, an independent chopper operating at the same frequency interrupted the probe radiation in the absence of the pump and the signal J^0_{pr} was recorded. In this way calculations yielded the quantity

$$L = \ln (J^0_{pr}/J_{pr}) = -\ln (1 - \Delta J^0_{pr}/J_{pr}). \quad (2)$$

Modulation of the probe radiation occurred mainly because of absorption by nonequilibrium EH pairs generated by the pump radiation. However, the value of L was affected by a number of different factors. Therefore, we had to establish experimentally the conditions under which analysis of the absorption of the probe radiation could be simplified sufficiently to be able to use the dependence $L(I)$ in order to determine the rate of generation of nonequilibriun EH pairs W as a function of I and to identify the mechanism of nonlinear absorption of the pump radiation.

One of these conditions was the exclusion of the effects nonlinear in the densities of free electrons $n = n_0 + \delta n$ and holes $p = p_0 + \delta p$ (n_0 and p_0 are the equilibrium densities). For this one must have $\delta n \ll n_0$ (in the case under discussion we have $\delta p = \delta n$, $p_0 \ll n_0$, δn). A second condition is associated with the need to reduce considerably the effects due to the nonlinear dependence of the pump intensity $I(z, t)$ in a sample on the intensity of the incident pump radiation I, which appears because of the absorption by nonequilibrium carriers.

At high intensities the carrier-density nonlinearity typical of multiphoton absorption involving free carriers can give rise to an exponential increase in the number of nonequilibrium EH pairs (see Ref. 9) and can even cause optical damage to a material. There are grounds for assuming that such a situation was encountered in Ref. 10, where a sharp reduction in the damage threshold of n-type GaAs ($n_0 \approx 10^{16}$ cm^{-3}) was found when the wavelength of the incident radiation was reduced from $\lambda = 10.6$ μm to $\lambda = 2.76$ μm. In the latter case the photon energy was $3\hbar\omega \approx 1.35$ eV ($E_g = 1.4$ eV).

These conditions were satisfied in our experiments. The relative modulation of the probe radiation flux was usually less than 0.2 and we also had $\delta n/n \lesssim 3.10^{-2}$. In this situation the value of L was proportional to the rate W of generation of EH pairs per unit volume. The value of L depended on the cross section for the absorption of light by free carriers and on the interband recombination time. These parameters varied with the temperature T of a sample. However, in the region of the three-photon absorption edge the most important factor was the dependence of the transition probability W_{cv} on T, which was due to the temperature dependence of E_g. Therefore, it is clear from the experimental data given below, that the change in L in a certain range of values of D was similar to the spectral dependence $W_{cv}(\omega)$.

Figure 1 shows the dependences $L(T)$ obtained by using two oppositely directed beams with the same photon energy $\hbar\omega_{pp,pr} = 0.117$ eV of the pump ("pp") and probe ("pr") beams in a sample of n-type InAs in which the density of free electrons was $n_0 = 1.5 \times 10^{16}$ cm^{-3} and the pump radiation had either linear or circular polarization. We included in Fig. 1 the dependence $\Lambda_{exp}(T)$ of the LCD parameter, which reached its maximum value (~ 10) at $T_0 = 296$ K. At this temperature the band gap was $E_g = 3\hbar\omega$ (Ref. 7). For $T < T_0$ the band gap E_g increased, but $L(T)$ did not approach zero, although in the region of the tail it decreases rapidly with increasing $\Delta_3 = E_g(T) - 3\hbar\omega$.

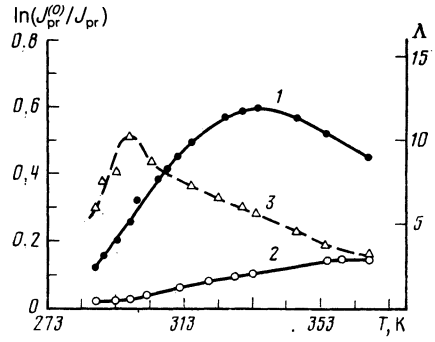

FIG. 1. Temperature dependences of $\ln(J^0_{pr}/J_{pr})_l$ (curve 1) and $\ln(J^0_{pr}/J_{pr})_c$ (curve 2) and of their ratio Λ_{exp} (3), obtained by the method of two oppositely directed beams reaching a sample of n-type InAs; $n_0 = 1.5 \times 10^{16}$ cm^{-3}, $\hbar\omega_{pp} = \hbar\omega_{pr} = 0.117$ eV.

Figure 2 contains log–log plots of $L(I)$ determined for several values of T at constant n_0 and $\hbar\omega$. In all cases the values of $L(I)$ could be approximated satisfactorily by dependences of the I^μ type. The straight lines in Fig. 2 had the slope of μ.

At $T = 298$ K both functions were cubic for linearly and circularly polarized pump radiations, in agreement with the fact that in this case we had $\Delta_3 < 0$ and direct interband three-photon transitions were possible. Lowering of T (corresponding to an increase in Δ_3) increased the slope of the

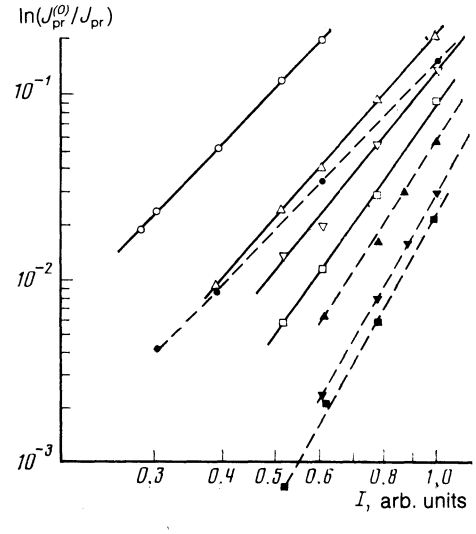

FIG. 2. Dependences of the values of $\ln(J^0_{pr}/J_{pr})$ on the intensity and polarization of the pump radiation obtained for different temperatures of a crystal T: ○), ●) 298 K; △), ▲) 273 K; ▽), ▼) 245 K; □), ■) 233 K. The filled symbols correspond to circularly polarized pump radiation and the open symbols to linearly polarized radiation; $\hbar\omega_{pp} = \hbar\omega_{pr} = 0.117$ eV, n-type InAs, $n_0 = 1.5 \times 10^{16}$ cm^{-3}, $d = 0.15$ cm.

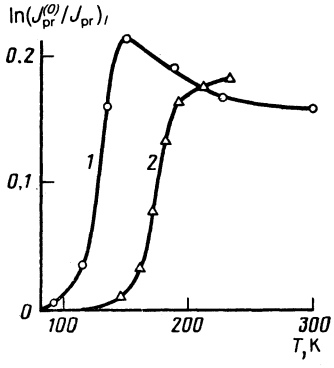

FIG. 3. Temperature dependence of $\ln(J_{pr}^0/J_{pr})_l$ obtained for a sample of n-type InAs: 1) $n_0 = 1.5\times10^{16}$ cm^{-3}; 2) $n_0 = 8\times10^{16}$ cm^{-3}.

curves. At $T = 273$ K ($\Delta_3 = 5.6$ meV) it was found that in the case of linearly polarized pump radiation the power exponent was $\mu_l = 3.3$, whereas for circularly polarized pump radiation it was $\mu_c = 4.65$. At $T = 245$ K ($\Delta_3 = 12.7$ meV) the corresponding values were $\mu_l = 3.6$ and $\mu_c = 5$; at $T = 233.5$ K ($\Delta_3 = 15.7$ meV), $\mu_l = 4.2$ and $\mu_c = 5$ were found.

The three-photon absorption edge of InAs was investigated at lower temperatures using a CO_2 laser line with $\lambda = 9.5\mu$m ($\hbar\omega = 0.131$ eV). The value $E_g = 3\hbar\omega$ was reached in this case at $T = 120$–130 K. In the least heavily doped samples the three-photon absorption edge should occur at these temperatures, according to the dependences $E_g(T)$ we obtained. In the case of more heavily doped samples it shifted because of the Moss–Burstein effect. This is demonstrated in Fig. 3, which gives the dependences of L on T obtained for $n_0 = 1.5\times10^{16}$ and 8×10^{16} cm^{-3}. Tails of multiphoton absorption appeared clearly in the range $\Delta_3 > 0$. In the case $\hbar\omega = 0.131$ eV we also obtained the $L(I)$ dependence. As in Fig. 2, in the investigated range of I they could be approximated satisfactorily by expressions of the I^μ type. For a sample with $n_0 = 1.5\times10^{16}$ cm^{-3} at $T = 295$ K the power exponent was 3 ($\Delta_3 < 0$), whereas at $T = 98$ K (linearly polarized pump radiation) it approached 4 (in this case we had $\Delta_3 \approx 7$ meV).

In the case of a more heavily doped sample ($n_0 = 8\times10^{16}$ cm^{-3}) the nature of this dependence was quite different. For example, for $T = 267.5$ K and $\hbar\omega = 0.117$ eV it was found that $\mu_l = 3$ for linearly polarized pump radiation. For the same values of n_0 and T the Fermi level was approximately 15 meV higher than the conduction band edge and the deficit was $\Delta_3 \approx 7.2$ meV. For circularly polarized pump radiation the cubic law representing the dependence $L(I)$ continued to hold in the range $T > 300$ K ($\hbar\omega = 0.117$ eV), whereas at $T = 255$ K the value of μ_c was already 5.

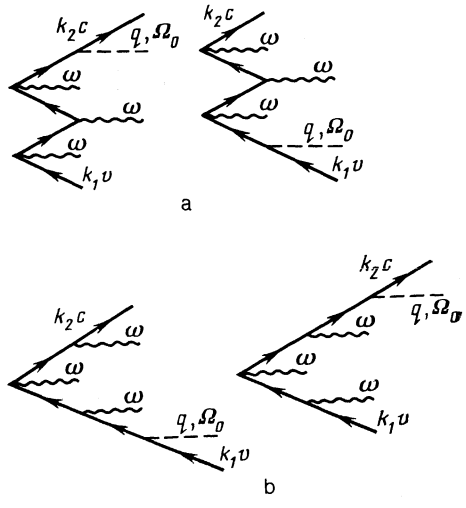

FIG. 4. Diagrams of matrix elements for three-photon transitions involving an optical phonon $M_{l(c)}^{(3)}$: a) linearly polarized radiation $M_l^{(3)}$; b) circularly polarized radiation $M_c^{(3)}$ (two diagrams are given; the other four are obtained by transposition of intraband and interband phonon vertices).

3. MULTIPHOTON INTERBAND TRANSITIONS INVOLVING AN OPTICAL PHONON

In this section we shall consider multiphoton transitions involving an optical phonon in direct-gap semiconductors in the case of linear and circular polarization of the pump radiation. We shall allow for the nonequilibrium of the phonon subsystem in the field of high-power radiation. This problem was solved in Ref. 11 for the case of the linear polarization of the radiation and an equilibriun phonon distribution function, but no allowance was made for the scattering of a hole from a virtual pair by a phonon. This introduced an error in the transition matrix element as a function of the phonon momentum q at low values of q.

The matrix elements $M_{\mathbf{k},\mathbf{q}}^{(s)}$ of an s-photon interband transition will be calculated in the $(s+1)$th order of perturbation theory: s orders with respect to the interaction of H_1 of the electron subsystem with strong optical radiation and one order with respect to the polarization interaction H_2 (PO interaction) with longitudinal optical phonons. Using the smallness of the ratios $\Delta_s/\hbar\omega$, we find that

$$\frac{(H_1)_{cc}}{(H_1)_{cv}} \approx \beta(k) = \left(\frac{\hbar^2k^2}{2m_rE_g}\right)^{1/2} \ll 1, \quad \frac{(H_2)_{cv}}{(H_2)_{cc}} \approx \beta(q) \ll 1, \tag{3}$$

[$m_r^{-1} = m_c^{-1} + m_v^{-1}$, q is the phonon wave vector, $(H_1)_{cc}$ are the "forbidden" intraband matrix elements, and $(H_1)_{cv}$ are the allowed interband matrix elements], we can readily identify the diagrams which make the principal contribution to $M_{\mathbf{k},\mathbf{q}}^{(s)}$. They are plotted in Figs. 4a and 4b for the case when $s = 3$. When linearly polarized radiation is absorbed, only the graphs with the interband phonon vertices remain in $M_{\mathbf{k},\mathbf{q}}^{(3)}$, whereas in the case of absorption of circularly polarized radiation the diagrams have one interband and two intraband phonon vertices, in agreement with the selection rules for this case.[3] To lowest order in the parameters $\beta(q)$, $\beta(k)$, and $(\Delta_3 + \hbar^2\mathbf{k}^2/2m_r)/\hbar\omega$, we obtain

$$M_{k,q(l)}^{(3)} = \Phi_{po}(q)\,[B_3(\mathbf{k}-\mathbf{q}) - B_3(\mathbf{k})]R_{3l}, \tag{4}$$

$$M_{k,q(c)}^{(3)} = -\Phi_{po}(q)\,[(\mathbf{e}(\mathbf{k}-\mathbf{q}))^2B_3(\mathbf{k}-\mathbf{q}) - (\mathbf{ek})^2B_3(k)]R_{3c} \tag{5}$$

where $\mathbf{e}$ is the polarization unit vector of the light,

$$\Phi_{p0}(q)=\frac{1}{q}\left[\frac{2\pi e^2\hbar\Omega_0 N(q,\Omega_0)}{\varepsilon^* V}\right]^{1/2},$$

$$B_3(\mathbf{k})=\left(\mathbf{k}^2+\frac{\bar{\Delta}_3}{1+\gamma}\right)^{-1},\quad \bar{\Delta}_3=\frac{2m_c\Delta_3}{\hbar^2},$$

$$R_{3c}=\frac{e^3A_0^3}{c^3(\hbar\omega)^2}\frac{(\mathbf{ep}_{cv})}{m_r m},\quad R_{3l}=\left(\frac{m_r}{m}\right)^2\frac{(\mathbf{ep}_{cv})^2}{2\hbar^2}R_{3c},$$

$$\varepsilon^{*-1}=\varepsilon_\infty^{-1}-\varepsilon_0^{-1},\quad \gamma=m_c/m_v, \tag{6}$$

V is the normalization volume, Ω_0 is the optical phonon frequency, A_0 is the amplitude of the vector potential of the electromagnetic wave $[I=n_\omega\omega^2A_0^2(2\pi c)^{-1}]$, ε_0 and ε_∞ are the static and high-frequency permittivities, and $N(q,\Omega_0)$ are the occupancy numbers of optical phonons.

In the case when the the phonon distribution function $N(q,\Omega_0)$ is almost isotropic and there is no degeneracy in the conduction and valence bands, we find that the probabilities of three-photon transitions involving the absorption of an optical phonon in the case of linearly polarized and circularly polarized pump radiations are given by the following expressions:

$$W_{po,l}^{(3)}=\frac{e^2}{\hbar\pi^2\varepsilon^*}|R_{3l}|^2\Phi_3,\qquad W_{po,c}^{(3)}=\frac{8m_c^2e^2\Omega_0^2}{15\hbar^3\pi^2\varepsilon^*}|R_{3c}|^2\Phi_1, \tag{7}$$

where

$$\Phi_i=\frac{\delta_0^{i-2}}{4\gamma}\int_0^{q_m}dqN(q,\Omega_0)G_i(\delta_0,q),\qquad \delta_0=\frac{2m_c\Omega_0}{\hbar}, \tag{8}$$

$$q_m=[(1+\gamma^{-1})(\delta_0-\bar{\Delta}_3)]^{1/2}. \tag{9}$$

The functions G_1 ($i=1$ or 3) on q are plotted in Fig. 5. For the LCD parameter we obtain from Eq. (7)

$$\Lambda_{p0}^{(3)}=\Lambda_0^{(3)}\frac{\Phi_3}{\Phi_1},\qquad \Lambda_0^{(3)}=\frac{15}{32}\frac{m_r^4}{m^4m_c^2}\frac{p_{cv}^4}{(\hbar\Omega_0)^2}. \tag{10}$$

At high pump intensities I the phonon distribution function $N(q,\Omega_0)$ depends on I. This is mainly due to the generation of nonequilibrium phonons in the course of relaxation of free electrons, which have absorbed a photon as a result of an indirect interband transition. We can find $N(q,\Omega_0)$ only if we know the electron distribution function $f_c(\mathbf{k})$. However, a rigorous calculation of $f_c(\mathbf{k})$ for the actual conditions in our experiments ($T\sim200$–300 K, $n_0\approx10^{16}$–10^{17} cm^{-3}, comparable electron–electron and electron–phonon collision frequencies) meets with considerable difficulties of fundamental and computational nature (various aspects of this problem are considered in Refs. 12–16). On the other hand, under these conditions it is unlikely that the distribution function should have any peaks of the type considered in Refs. 14–16. Therefore, to interpret qualitatively the observed dependence of the effect on Δ_3, I, and n_0 it is sufficient to replace $f_c(\mathbf{k})$ with the Boltzmann distribution characterized by an electron temperature T_e which increases with I. Then, $N(q,\Omega_0)$ is given by[17,18]

$$N(q,\Omega_0)=[N_0+\tau\omega_1Z(q)]\left\{1+\left[\exp\left(\frac{\hbar\Omega_0}{T_e}\right)-1\right]\tau\omega_1Z(q)\right\}^{-1}, \tag{11}$$

$$Z^{-1}(q)=\left(\frac{q}{q_{\Omega_0}}\right)^3\left(\frac{T_e}{\hbar\Omega_0}\right)^{1/2}\exp\left\{\frac{m_c\Omega_0^2}{2q^2T_e}+\frac{\hbar^2q^2}{8m_cT_e}+\frac{\hbar\Omega_0}{2T_e}\right\}, \tag{12}$$

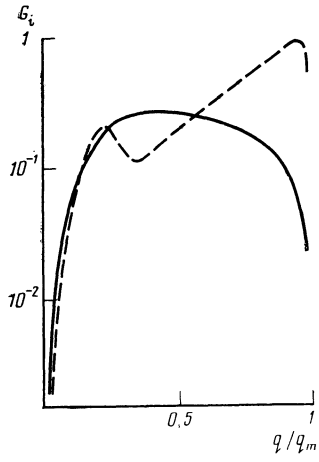

FIG. 5. Probabilities $G_i(q,\Delta_3)$ of three-photon transitions involving an optical phonon plotted against the phonon wave vector q. The continuous curve corresponds to $i=1$ (circular polarization) and the dashed curve corresponds to $i=3$ (linear polarization); $\Delta_3=5$ meV.

$$\omega_1=\frac{\pi^{3/2}n_0e^2}{\varepsilon^*m_c\Omega_0},\qquad q_{\Omega_0}=\delta_0^{1/2}, \tag{13}$$

where τ^{-1} is the frequency of phonon–phonon collisions and N_0 is the equilibrium distribution function of optical phonons.

It is clear from Eqs. (11)–(13) that $N(q,\Omega_0)$ has an extremum (a maximum for $T_e>T$ and a minimum for $T_e<T$) when $q=q_0$, where

$$q_0^2=\frac{2m_cT_e}{\hbar^2}\left\{\left[9+\left(\frac{\hbar\Omega_0}{T_e}\right)^2\right]^{1/2}-3\right\}. \tag{14}$$

For both $q\gg q_0$ and $q\ll q_0$, we have $N(q,\Omega_0)\approx N_0$. It is clear from Eq. (8) that Φ_i increases with the electron temperature T_e. The rate of this increase rises as the deficit Δ_3 increases. The reason is that as Δ_3 increases there is a reduction in the maximum wave vector q_m of the phonons which can still participate in the process. When Δ_3 is not too close to $\hbar\Omega_0$, we have $q_m\gg q_0$. On reduction in q_m the contribution of short-wavelength phonons with $q\gg q_0$, whose distribution function is close to equilibrium, drops out. There is a corresponding increase in the relative contribution of nonequilibrium phonons with $q\sim q_0$, which results in a faster rise of Φ_i with T_e (and, consequently, with I) at high values of Δ_3 (see Fig. 7 below).

It is clear from Fig. 5 that the integral Φ_3 includes a major contribution from the range $q\sim q_m$, where $N(q,\Omega_0)\approx N_0$ whereas the integral Φ_1 includes a contribution from the smaller values $q\sim q_0$, where $N(q,\Omega_0)$ is far from N_0. Consequently, for a fixed value of Δ_3 the function Φ_1, governing the rate of three-photon transitions involving an optical phonon in the case of circularly polarized pump radiation, rises as a function of T_e and I more rapidly than does the function Φ_3 in the case of linear polarization of the pump radiation (see Fig. 7 below). The LCD parameter $\Lambda_{p0}^{(3)}$ for this three-photon transition mechanism increases as Δ_3 is reduced (a numerical estimate for $I=1$ MW/cm^2 shows that $\Lambda_{p0}^{(3)}$ increases by a factor of 1.6 as Δ_3 is reduced from 15 to 5 meV: without allowance for relaxation we find $\Lambda_{p0}^{(3)}\to\infty$ in the limit $\Delta_3\to0$). On the other hand, it is clear from Eqs.

(11)–(13) that the dependence $\Phi_i(T_e)$ [and, consequently, $\Phi_i(I)$] becomes somewhat stronger as the free electron density n_0 increases. The conflict between this conclusion and the experimental results (Sec. 2) shows that indirect phonon-assisted three-photon transitions cannot be explained by just one mechanism if all the experimental results are to be accounted for.

4. MULTIPHOTON INTERBAND TRANSITIONS INVOLVING FREE ELECTRONS

The probabilities of s-photon ($s = 2$ and 3) transitions $W^{(s)}_{ee,l(c)}$ involving free carriers were calculated in Ref. 19. An allowance was made only for the contribution of the electrons in the energy range $\hbar\Omega_0 < E < E_1 \approx \hbar\omega$ representing electrons arriving from the bottom of the conduction band due to energy acquired as a result of indirect intraband absorption and subsequent relaxation. The case when the main energy loss channel in this range of energies is the emission of optical phonons and the distribution function of electrons is of non-Boltzmann type was considered in Ref. 19. When the pump radiation is circularly polarized there is an important contribution also from the range of higher energies which is reached by electrons as a result of two-photon or cascade one-photon transitions in the conduction band. It follows from the laws of conservation of energy and momentum that electrons of energies $E > E_{min} = (2\gamma + 1)(\gamma + 1)^{-1}\Delta_s$ can participate in this process. The main contribution to the cross section of the process comes from electrons with high energies, which can transfer momentum in small portions to the newly created pair:

$$q \gtrsim q_{min} = \frac{\Delta_s}{\hbar}\left(\frac{m_c}{2E}\right)^{1/2}. \tag{15}$$

At low temperatures such that $T < \Delta_s$ or $\Delta s \gtrsim \hbar\Omega_0$ the process is actually dominated by electrons from the non-Boltzmann "tail" of the distribution function with energies $E > \hbar\Omega_0$. However, under the conditions in our experiments when $\Delta_3 \lesssim \hbar\Omega_0/2$, the temperature is of the order of the room value and $n_0 \sim 10^{16}$–10^{17} cm^{-3}, so that the role of the non-Boltzmann correction diminishes. Therefore, although the results of Ref. 19 do agree qualitatively with the nonlinear absorption in n-type InAs, they are insufficient to interpret the experimental results. It is useful to consider also a case which is in a sense opposite, when the process of energy relaxation involves mainly electron–electron collisions and $f_c(\mathbf{k})$ can be approximated throughout the investigated range of energies by the Boltzmann distribution with an electron temperature T_e that depends on I.

The probabilities of three-photon transitions involving free electrons in a nondegenerate semiconductor are described by

$$W^{(3)}_{ee,c} = \frac{2^{3/2}\cdot 3e^4 m_c^{1/2}}{\varepsilon_0^2\hbar^{5/2}\pi^3\Omega_0^{1/2}}|R_{3c}|^2 F_3, \tag{16}$$

$$W^{(3)}_{ee,c} = \frac{2^{9/2}e^4 m_c^{5/2}\Omega_0^{3/2}}{5\varepsilon_0^2\pi^3\hbar^{9/2}}|R_{3c}|^2 F_1,$$

where R_{3l} and R_{3c} are given by the expressions in Eq. (6), and

$$F_i = \int_{k_{min}}^{\infty} dk_0 k_0^2 f_c(k_0) P_i(k_0, \Delta_3), \qquad k_{min}^2 = 2m_c E_{min}/\hbar^2. \tag{17}$$

The explicit expressions for the functions $P_i(k_0, \Delta_3)$ in the integrands are given in Refs. 9 and 19 and are very cumbersome.

In the case of the Boltzmann distribution function it follows from Eq. (17) that the $F(T_e)$ contain regions of slow and fast variation. This is due to two different factors, which are responsible for the rise of F_i with increasing T_e. The first of these, an increase in the number n_1 of electrons of energies $E > E_{min}$, predominates at low values of $T_e < \Delta_3$. Then n_1 rises exponentially, which corresponds to the region of rapid variation of $F_i(T_e)$. At higher values of T_e the rise of n_1 slows down (we now have $n_2 = n_0 - n_1 \ll n_1$) and the second factor, which is an increase in the matrix element of a transition on increase in the energy of a stimulating electron, begins to play the major role. This process can be described by a power law, which corresponds to the region of relatively slow variations of F_i. Clearly, at high values of Δ_3 the first of these factors predominates at values of T_e which are higher than when Δ_3 is low. Therefore, if we select a fixed temperature interval ΔT_e, then the rate of variation in this interval $F_i(T_e)$ increases with Δ_3.

The function $F_1(T_e)$ rises more rapidly with T_e than does $F_3(T_e)$. This occurs because in view of the strong "forbiddenness of the transition in the case of linear polarization of the pump radiation the function P_1 varies more rapidly than P_3 as a function of the momentum k_0 of the stimulating electron, and in the integral F_1 the range of higher values of k_0 makes a relatively larger contribution than to F_3 [in the case of high values of k_0 the function $f_c(k_0)$ varies with temperature more rapidly than at low values of k_0]. The LCD parameter $\Lambda^{(3)}_{ee}$ for three-photon transitions involving free electrons increases as Δ_3 is reduced [an estimate gives $\Lambda^{(3)}_{ee}(5\ \text{meV})/\Lambda^{(3)}_{ee}(15\ \text{meV}) \sim 4.7$ for $I = 1$ MW/cm^2]. These features of the behavior of $F_i(T_e, \Delta_3)$ are illustrated in Figs. 6 and 7.

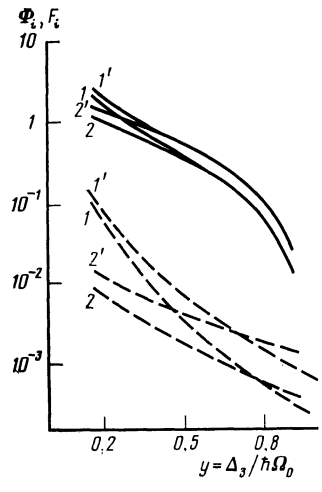

FIG. 6. The functions $\Phi_i(\Delta_3, T_e)$ and $F_i(\Delta_3, T_e)$, governing the probabilities of three-photon transitions involving an optical phonon and free electrons, plotted versus the deficit Δ_3. The continuous curves give Φ_i and the dashed curves give F_i. The number 1 represents $i = 3$ (linear polarization) and the number 2 represents $i = 1$ (circular polarization). The numbers without primes correspond to $T_e = 300$ K, whereas those with primes correspond to $T_e = 500$ K. The parameter $\gamma = 0.0575$ corresponds to a transition from the heavy-hole subband; $\tau\omega_i = 5.71$.

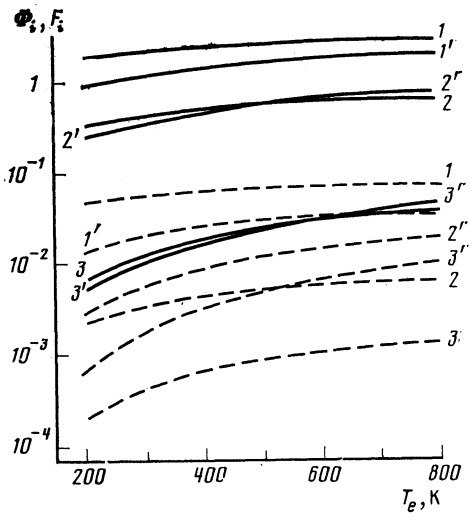

FIG. 7. The functions $\Phi_i(\Delta_3, T_e)$ and $F_i(\Delta_3, T_e)$, governing the probabilities of three-photon transitions involving an optical phonon and free electrons, plotted against the electron temperature T_e. The continuous curves represent Φ_i and the dashed curves correspond to F_i. The numbers 1, 2, and 3 correspond to $\Delta_3 = 5$, 14.6, and 27.3 meV, respectively. The numbers without a prime represent the $i = 3$ case (linear polarization), whereas those representing $i = 1$ are marked with a prime (circular polarization). The parameter $\gamma = 0.0575$ corresponds to transition from the subband of heavy holes and $\tau\omega_1 = 5.71$.

5. CONCLUSIONS

These theoretical ideas make it possible to explain practically all the qualitative features of the investigated processes manifested in our experiments.

We shall list once again the main qualitative results of our investigation.

1. First of all, the direct four-photon generation of EH pairs is not manifested under our experimental conditions. This follows from the strong dependence of the effect on Δ_3 (Fig. 1), which should not occur in the case of direct four-photon transitions at $(-\Delta_4 \sim \hbar\omega$, and also from estimates of the amplitudes of the probabilities deduced using results from Refs. 4, 5, and 20. On the other hand, the rapid increase in the probabilities of transitions as the deficit Δ_3 is reduced and a similar behavior of the LCD parameter $\Lambda^{(3)}$ (Fig. 1) are typical precisely of three-photon transitions involving a phonon or free electrons.

2. In the case of linear and circular polarizations of the pump radiation the rate of generation of EH pairs increases on increase of the intensity at high values of Δ_3 faster than for low values of Δ_3, which can be explained qualitatively as follows: an increase in Δ_3 increases the minimum kinetic energy $E_{\min}$ of an electron and reduces the maximum wave vector q_m of a phonon stimulating indirect multiphonon transitions. In the former case this results in a change to exponential variation of the function $F_i(T_e)$ and, consequently, of $F_i(I)$. In the latter case there is an increase in the relative contribution of nonequlibrium phonons, the number of which increases on increase in the intensity I.

3. If $\Delta_3 > 0$, then in the case of circular polarization the increase in the rate of generation of EH pairs on increase in the intensity I is faster for the circular than for the linear polarization case. This is due to the fact that in view of the forbiddenness of three-photon transitions in the case of circularly polarized light, their component matrix elements depend more strongly on the energy than in the linear polarization case and this, as already pointed out, increases the relative contribution of nonequilibrium phonons and electrons.

4. These ideas also provide the basis for a qualitative explanation of the experimentally observed carrier-density dependence: at low values of Δ_3 ($\sim$5–7 meV) the dependence of the rate of generation of EH pairs on I in the case of linearly polarized radiation is weaker for high values of n_0 (Sec. 2). This occurs because of a change in the absorption mechanism. For $n_0 = 1.5\times10^{16}$ cm^{-3} the *PO* mechanism still predominates. If it had continued to play the main role also at higher values of n_0, the dependence $W(I)$ would have become steeper. However, an increase in n_0 increases the role of the electron–electron (*ee*) collision mechanism which in the case of such low values of the deficit is characterized by a dependence close to $W_{ee}^{(3)} \propto I^3$ (almost all free electrons may participate in the process). It is just this dependence which is observed for $n_0 = 8\times10^{16}$ cm^{-3}. It agrees with a theoretical estimate of the probabilities of three-photon transitions obtained for both mechanisms of indirect transitions. They show that the *PO* mechanism predominates in the range $n_0 \lesssim 10^{16}$ cm^{-3}. For $n_0 \gtrsim 10^{17}$ cm^{-3}, the *ee* mechanism predominates and in the range 10^{16} cm^{-3} $n_0 \lesssim 10^{17}$ cm^{-3} both mechanisms make comparable contributions.

[1)] A more detailed description of the experimental conditions and of the results obtained can be found in Ref. 9.

[1]A. M. Danishevskiĭ, E. L. Ivchenko, S. F. Kochegarov, and M. I. Stepanova, Pis'ma Zh. Eksp. Teor. Fiz. **17**, 181 (1973) [JETP Lett. **17**, 129 (1973)].

[2]E. V. Beregulin, D. P. Dvornikov, E. L. Ivchenko, and I. D. Yaroshetskiĭ, Fiz. Tekh. Poluprovodn. **9**, 876 (1975) [Sov. Phys. Semicond. **9**, 576 (1975)].

[3]E. L. Ivchenko and E. Yu. Perlin, Fiz. Tverd. Tela (Leningrad) **15**, 2781 (1973) [Sov. Phys. Solid State **15**, 1850 (1974)].

[4]E. Yu. Perlin, V. A. Kovarskiĭ, and V. N. Chebotar', Fiz. Tverd. Tela (Leningrad) **18**, 239 (1976) [Sov. Phys. Solid State **18**, 137 (1976)].

[5]E. Yu. Perlin and V. N. Chebotar', *Kinetics of Nonequilibrium Electrons and Electron–Vibrational Systems* [in Russian], Shtiintsa, Kishinev (1982), p. 83.

[6]A. M. Danishevskiĭ, S. F. Kochegarov, and V. K. Subashiev, Zh. Eksp. Teor. Fiz. **70**, 158 (1976) [Sov. Phys. JETP **43**, 83 (1976)].

[7]S. B. Arifzhanov, A. M. Danishevskiĭ, E. L. Ivchenko, S. F. Kochegarov, and V. K. Subashiev, Zh. Eksp. Teor. Fiz. **74**, 172 (1978) [Sov. Phys. JETP **47**, 88 (1978)].

[8]D. P. Dvornikov, E. L. Ivchenko, and I. D. Yaroshetskiĭ, Fiz. Tekh. Poluprovodn. **12**, 1571 (1978) [Sov. Phys. Semicond. **12**, 927 (1978)].

[9]A. M. Danishevskiĭ, S. F. Kochegarov, E. Yu. Perlin, *et al.*, Preprint No. 908 [in Russian], Ioffe Physicotechnical Institute, Academy of Sciences of the USSR, Leningrad (1984).

[10]A. V. Sidorin, Tr. Fiz. Inst. Akad. Nauk SSSR **137**, 135 (1982).

[11]I. A. Chaĭkovskiĭ, Fiz Tekh. Poluprovodn. **6**, 229 (1972) [Sov. Phys. Semicond. **6**, 198 (1972)].

[12]V. F. Gantmakher and I. B. Levinson, *Scattering of Carriers in Metals and Semiconductors* [in Russian], Nauka, Moscow (1984).

[13]I. N. Yassievich and I. D. Yaroshetskiĭ, Fiz. Tekh. Poluprovodn. **9**, 857 (1975) [Sov. Phys. Semicond. **9**, 565 (1975)].

[14]F. T. Vas'ko and Z. S. Gribnikov, Pis'ma Zh. Eksp. Teor. Fiz. **21**, 629 (1975) [JETP Lett. **21**, 297 (1975)].

[15]S. E. Kumekov and V. I. Perel', Pis'ma Zh. Eksp. Teor. Fiz. **39**, 379 (1984) [JETP Lett. **39**, 456 (1984)].

[16]S. É. Esipov and I. B. Levinson, Zh. Eksp. Teor. Fiz. **86**, 1915 (1984) [Sov. Phys. JETP **59**, 1113 (1984)].
[17]V. L. Gurevich and D. A. Parshin, Zh. Eksp. Teor. Fiz. **72**, 1589 (1977) [Sov. Phys. JETP **45**, 834 (1977)].
[18]L. E. Vorob'ev, Fiz. Tekh. Poluprovodn. **8**, 1291 (1974) [Sov. Phys. Semicond. **8**, 839 (1975)].
[19]E. Yu Perlin A. V. Fedorov, and M. B. Kashevnik, Zh. Eksp. Teor. Fiz. **85**, 1357 (1983) [Sov. Phys. JETP **58**, 787 (1983)].
[20]V. A. Kovarskiĭ and E. Yu. Perlin, Fiz. Tverd. Tela (Leningrad) **13**, 1217 (1971) [Sov. Phys. Solid State **13**, 1013 (1971)].

Translated by A. Tybulewicz